# Explicit Computations of the Frozen Boundaries of Rhombus Tilings of Polygonal Domains

Arthur Azvolinsky
Council Rock High School South

February 12, 2016

**Abstract**

Consider a polygonal domain $\Omega$ drawn on a regular triangular lattice. A *rhombus tiling* of $\Omega$ is defined as a complete covering of the domain with $60^{\circ}$-rhombi, where each one is obtained by gluing two neighboring triangles together.

We consider a uniform measure on the set of all tilings of $\Omega$. As the mesh size of the lattice approaches zero while the polygon remains fixed, a random tiling approaches a deterministic limit shape. An important phenomenon that occurs with the convergence towards a limit shape is the formation of *frozen facets*; that is, areas where there are asymptotically tiles of only one particular type. The sharp boundary between these ordered facet formations and the disordered region is a curve inscribed in $\Omega$. This inscribed curve is defined as the *frozen boundary*.

The goal of this project was to understand the purely algebraic approach, elaborated on in a paper by Kenyon and Okounkov, to the problem of explicitly computing the frozen boundary. We will present our results for a number of special cases we considered.

## 1 Introduction

The notion of the tiling model provides the basis for this project. Let $\Omega$ be a polygonal domain drawn on a regular triangular lattice $T$. A *rhombus tiling* is a complete covering of a domain by pairs of neighboring triangles glued together, where each glued pair is called a *rhombus tile* (also known as a *lozenge*). See Figures 1 and 2 for examples. We will call a domain that can be completely covered by tiles *tilable*.

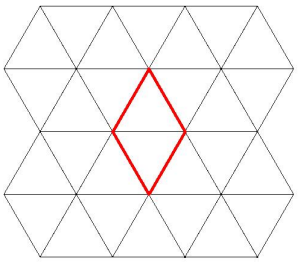

Figure 1: A Rhombus Tile from Two Adjacent Triangles of $T$

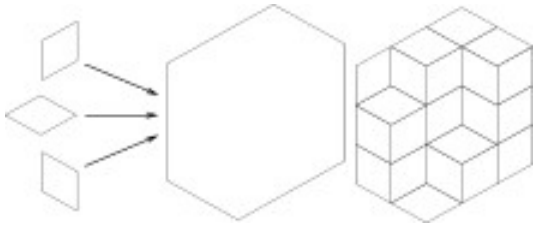

Figure 2: An Example of a Tiling[1]

If we examine random tilings of a given tilable domain as the lozenges get smaller and smaller, we encounter an important phenomenon: the formation of a deterministic limit shape [3, 12, 13].

One of the limit shape's interesting features is the formation of *frozen facets*; that is, zones inside the considered domain where there are asymptotically rhombi of only one particular type. There also exists a connected, open liquid region inside the domain, where there are asymptotically an arbitrary configuration of tiles. The curve that separates the liquid region from the frozen zones is called the *frozen boundary*, of which Theorem 3.1 from Section 3 gives a formal definition. See Figure 3 for an example of the convergence towards a frozen boundary. The main purpose of this project is to explicitly compute the frozen boundary for various tilable domains, using a purely algebraic approach from [12].

[1]This picture is borrowed from [6]

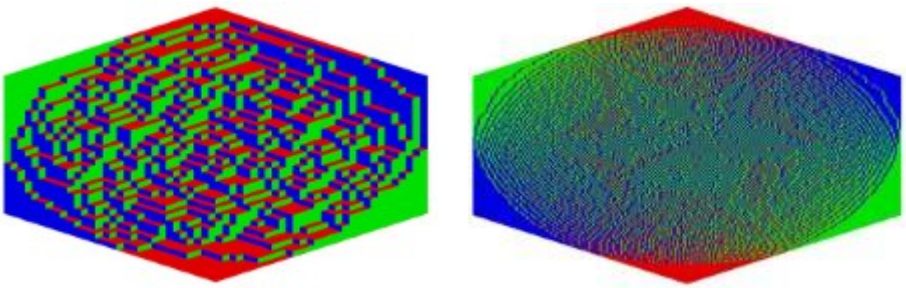

(a) Tiling of a Hexagon with Small Tile Size

(b) Tiling of a Hexagon with Smaller Tile Size

Figure 3: An Example of the Convergence Towards a Frozen Boundary[2]

The first examples presented in this paper will be computational results and algorithms with elliptical frozen boundaries in specific types of hexagons and with cardioidal frozen boundaries in specific types of octagons.

The hexagons we will consider are those that are equiangular and with 3 sets of parallel, equal sides. They must also have sides such that the lengths of any two yield a rational quotient. See Figures 2 and 3 above for examples of such hexagons. Section 4.1 elaborates on the set of hexagons considered in our computations.

The octagons we will consider in our computations are those that are derived from removing a rhombus from a hexagon with two different side lengths, as shown in Figure 4. Section 4.2 elaborates on the set of octagons considered in our computations.

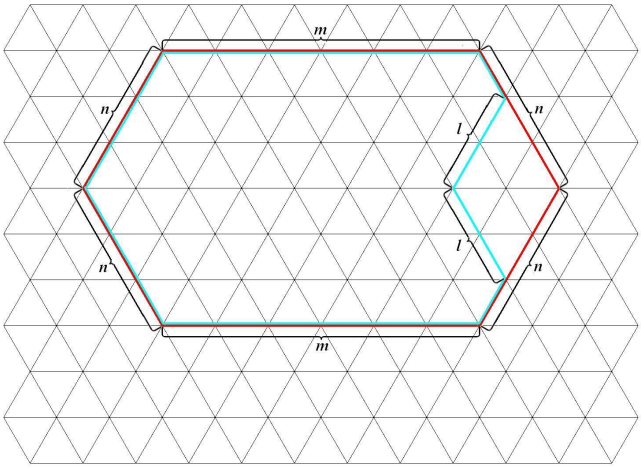


Figure 4: The Construction of a Considered Octagon

[2]These pictures are borrowed from [6]

After examples with hexagons and octagons, this paper will elaborate on results with 3-tangent and 4-tangent frozen boundaries as well as on a generalization to an $n$-tangent frozen boundary.

Figure 5 shows the process for constructing considered domains with such frozen boundaries. A domain with a 3-tangent frozen boundary is outlined in black, while the addition outlined in orange creates a domain with a 4-tangent frozen boundary. Successful additions (outlined in different colors) create domains with $n$-tangent frozen boundaries (where $n \geq 3$ for the domains in Figure 5). We will consider all domains geometrically similar to these ones. Sections 5 and 6 elaborate on such domains, and the computation of the frozen boundary for them was first obtained by L. Petrov in [18], using an approach different from the one in this paper.

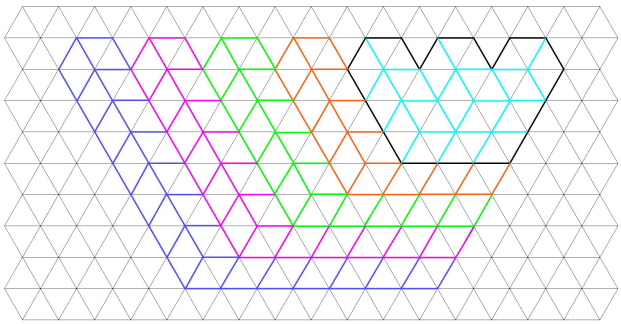

Figure 5: Construction of Domains with $n$-tangent Frozen Boundaries

We have developed algorithms for the computation of the frozen boundaries of all of the aforementioned domains. We have also developed visual results of the frozen boundaries contained in specific examples for each type of domain. See Figure 6 below for some of these results.

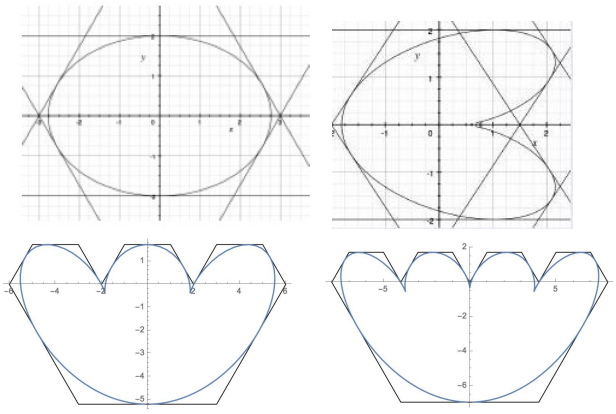

Figure 6: Examples of Visual Results

## 1.1 Road Map

**Section 2**

This section discuss various interpretations of the tiling model as well as the motivation for and applications of this concept.

**Section 3**

This section explains the 4 properties of the frozen boundary that give it uniqueness. It also elaborates on the concept of curve duality, which is central to two of the properties.

**Section 4**

This section presents results with a set of considered tilable hexagons and their elliptical frozen boundaries. It also presents results with a set of considered tilable octagons with their cardioidal frozen boundaries.

**Section 5**

This section presents a result with a frozen boundary that is a 3-tangent curve and elaborates on the algorithm used to obtain this result. The algorithm is also used to compute the frozen boudaries that are 3-tangent curves for a set of considered tilable domains.

**Section 6**

This section presents a result with a frozen boundary that is a 4-tangent curve and elaborates on the algorithm used to obtain this result. The algorithm is also used to compute the frozen boudaries that are 4-tangent curves for a set of considered tilable domains. This section also elaborates on the process for developing an algorithm for an $n$-tangent curve.

# 2 Background

## 2.1 Various Interpretations of the Tiling Model

One interpretation of the tiling model involves the notion of the perfect matching. A *perfect matching* of a graph $G$ is defined as a subset of edges that cover each vertex exactly once (see Figure 7 for an example, where the bolded edges are the ones in the perfect matching).

We will now explain how the tiling model relates to the concept of perfect matchings. Let $T_D{}^*$ be the dual graph to $T_D$, where $T_D \subset T$ such that $T_D$ and $\Omega$ completely cover each other. Each tiling of $\Omega$ corresponds to a perfect matching of $T_D{}^*$. The vertex that corresponds to the outer face of $T_D$ is excluded in $T_D{}^*$, along with all of the edges connected to that vertex. In this way, $T_D{}^*$ is always a subset of the infinite hexagonal (honeycomb) lattice. See Figure 8a for an example of $T_D$ and $T_D{}^*$ for a 10-gonal domain.

In this way, we have a bijection between the set of lozenges that make up a tiling of $\Omega$ and the set of edges of the corresponding perfect matching of $T_D{}^*$

(see Figure 8b). In this way, there is also a bijection between the tilings of $\Omega$ and the perfect matchings of ${T_D}^*$.

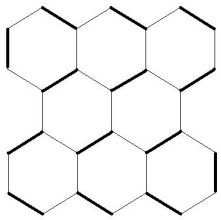

Figure 7: An Example of a Perfect Matching

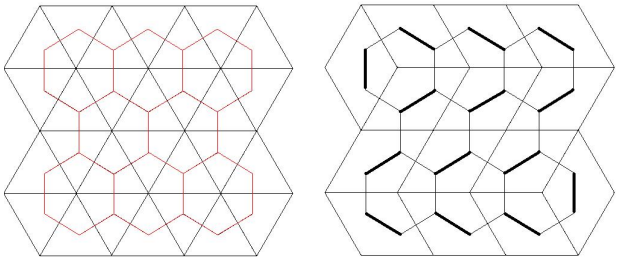

(a) Dual Graphs for a 10-gonal Domain

(b) A Tiling and its Corresponding Perfect Matching

Figure 8: The Duality of Tilings and Perfect Matchings

The height function offers another interpretation of the tiling model. If we color the inner faces of $T_D$ black and white so that no two adjacent faces are the same color, we can then orient the edges of black faces in a clockwise manner and the edges of white faces in a counterclockwise manner. We can then recursively define the height function $h^{T_D}$ [21], which assigns an integer to each vertex, as follows:

- Choose a vertex $v_0$ and set $h^{T_D}(v_0) = 0$
- For every edge $uv$ of a rhombus tile in a tiling, $h^{T_D}(v) - h^{alT_D}(u) = 1$, where the direction of edge orientation is from u to v.

See Figure 9 for an example of the implementation of the height function. Notice how the tiles, when colored in with 3 different colors in conjunction with the vertices numbered from the height function, create a 3-dimensional interpretation of the tiling model. This interpretation is known as a *stepped surface*.

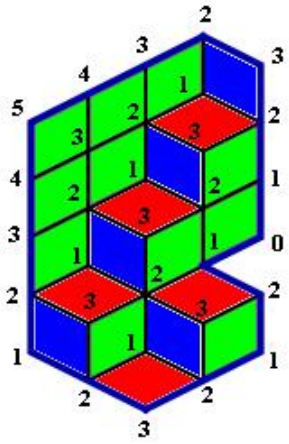

Figure 9: An Example of the Implementation of the Height Function[3]

### 2.2 Motivation

In physics, perfect matchings are known as dimer configurations, and in chemistry, they are known as Kekule structures. The molecules and atoms of matter are arranged on a crystal lattice. The arrangement of these particles on a lattice is of great interest in physics, prompting exploration in the theory of graphs and matchings. For example, the hexagonal structure of graphite may be represented by the honeycomb lattice, where each vertex corresponds to a carbon atom and each edge corresponds to a bond [9, 15].

A dimer is a molecule consisting of two bonded atoms. Examples include $H_2$ and $O_2$ gas. The dimer model is a statistical mechanics model introduced to represent the adsorption of diatomic molecules on crystal surfaces [11]. Since its success in modeling the behavior of partially dissolved crystals in equilibrium, it has been used to describe many other physical systems.

Thus, because tiling models have a bijectional relationship with perfect matchings (dimer configurations), they are a field of great interest in the context of their physical applications. See [1, 4, 8, 14, 23, 24] for elaboration on applications such as these as well as on many others.

## 3 Properties of the Frozen Boundary

The frozen boundary in our case is formally defined as follows:

**Theorem 3.1.** [3, 12] *Let $\Omega$ be a tilable, connected polygon with $3d$ sides. Fix $\epsilon > 0$. Consider the tilings of $\Omega$ by rhombi of size $\frac{1}{N}$. Then for sufficiently large $N$ all but an $\epsilon$ fraction of the tilings will have a temperate zone whose boundary*

[3]This picture is borrowed from [19]. We have colored it in and numbered the vertices.

*stays uniformly within distance $\epsilon$ of an inscribed curve. This inscribed curve is called the* frozen boundary*.*

A paper by Kenyon and Okounkov [12] gives 4 properties of the frozen boundary that make this definition unique (Theorems 3 and 4 from the paper). We can use these properties to accomplish our goal of explicitly computing the frozen boundary. They are as follows:

1. The frozen boundary is a curve inscribed in the related domain.
2. The frozen boundary is a rationally parameterizable (an algebraic curve with genus zero).
3. For a domain with $3d$ edges, the dual curve of the frozen boundary has degree $d$.
4. The dual curve of the frozen boundary is a winding curve.

The rest of this section will be devoted to elaboration on these properties.

## 3.1 Properties 1 and 2

Properties 1 and 2 are grouped together because unlike Properties 3 and 4, they do not require an understanding of the notion of curve duality, which is explained in the next subsection.

Theorem 3.1 above already articulates Property 1. In order to understand Property 2, we need to define rational parametrization:

**Definition 3.2.** [20] We will say that a real algebraic curve $C$ defined by the square-free equation $f(x, y) = 0$ is *rationally parametrizable* if there exist rational functions $x(t)$ and $y(t)$ (i.e. both can be represented in the form $\frac{P(t)}{Q(t)}$, where $P(t)$ and $Q(t)$ are polynomials in $t$) such that

1. for almost all $t_0 \in \mathbb{R}$ (i. e. for all but a finite number of exceptions), the point $(x(t_0), y(t_0)) \in C$, and
2. for almost every point $(x_0, y_0) \in C$, there exists a $t_0 \in \mathbb{R}$ such that $(x(t_0), y(t_0)) = (x_0, y_0)$

The parametrization of $C$ with $x = x(t)$ and $y = y(t)$ is known as the *rational parametrization* of $C$. We say that an algebraic curve with a rational parameterization is *rational* or with *genus zero* (they are all equivalent designations).

We have now explained Properties 1 and 2. For Properties 3 and 4, however, we need to first introduce the concept of curve duality.

## 3.2 Curve Duality

For this section, we will be working with real algebraic curves on the plane. There are several realizations of the dual to an algebraic curve. We will first examine the geometric realization, starting with defining reciprocation about the unit circle.

**Definition 3.3.** Let $C$ be a unit circle centered at the origin $O$. Let $P$ be any point in the plane of $C$ with distance $d > 0$ from $O$. Draw line $l$ perpendicular to line $OP$ and on the opposite side of $O$ so that $d * d' = 1$, where $d'$ is the distance from $l$ to $O$. $l$ is defined as the *reciprocal* of $P$ about the unit circle, and $P$ is also the reciprocal of $l$ about the unit circle. The reciprocal of a point $P$ at $O$ is a line at an infinite distance away from $O$, and the reciprocal of a line $l$ passing through $O$ is a point infinitely far away from $O$ and on the line perpendicular to $l$.

In more specific terms, the reciprocal of a point is known as its *polar*, and the reciprocal of a line is known as its *pole*. We will use the function rec($x$) to indicate the reciprocal of a point or line $x$. Now, we can use this definition of reciprocation about the unit circle to define the notion of a dual curve.

**Definition 3.4.** Let $C$ be an algebraic curve. Then the *dual curve* $C^*$ is defined as the set of poles of all the tangent lines to $C$.

An algebraic definition of the dual curve will be cardinal in the computations to come. In order to create this realization, parametric equations will be used. The following proposition is from [5].

**Proposition 3.5.** *Let $C$ be an algebraic curve given by the parametric equations $(u(t), v(t))$. Then $C^*$ has parametric equations*

$$\left(\frac{v'(t)}{u'(t)v(t) - v'(t)u(t)}, \frac{-u'(t)}{u'(t)v(t) - v'(t)u(t)}\right).$$

*Proof.* We will present the proof of this proposition for the reader's convenience (see [16] for the source of the proof).

Let us first determine the pole of the line $l$ given by $ax+by+1 = 0$. The claim is that it is $P(a, b)$. In order to show this, we need to prove three statements:

1. $P$ lies on the line $l'$ perpendicular to $l$ and passing through $O$.
2. $P$ and $l$ are on opposite sides of the origin $O$.
3. $d * d' = 1$, where $d = OP$ and $d'$ is the distance from $l$ to $O$.

The first statement can be shown to be true by examining the slopes of $l$ and $l'$. From the equation of $l$, its slope is -$\frac{a}{b}$. Since $l'$ passes through $O(0, 0)$ and $P(a, b)$, its slope is $\frac{b}{a}$. Because the slopes of $l$ and $l'$ are negative reciprocals, the two lines are perpendicular.

For the second statement, we can see that the axis intercepts of $l$ are the points $(-\frac{1}{a}, 0)$ and $(0, -\frac{1}{b})$. Since the nonzero $x$ and $y$ coordinates of the axis intercepts have opposite signs than the corresponding coordinates of $P(a, b)$, $P$ and $l$ are on opposite sides of $O$.

All that remains is to prove the third statement. We know that $d = \sqrt{a^2 + b^2}$. Since the distance from a point $(x_o, y_o)$ to line $l$ is $\frac{|ax_o+bx_o+c|}{\sqrt{a^2+b^2}}$, $d' = \frac{1}{\sqrt{a^2+b^2}}$. Hence, $d * d' = 1$.

We have proven the following:

$$\text{rec}(l) = P, \tag{1}$$

where $l$ is the line $ax + by + 1 = 0$ and $P = (a, b)$.

Note that we have also proven that $\text{rec}(P) = l$, by the definition of reciprocation.

Now we will consider the algebraic curve C with parametric equations $(u(t), v(t))$. Let us calculate a tangent line to C at a point $(u(t_o), v(t_o))$ on C. Using the derivative yields $y - v(t_o) = \frac{v'(t_o)}{u'(t_o)}(x - u(t_o))$. Expanding and rearranging, we have:

$$\frac{v'(t_o)}{v(t_o)u'(t_o) - u(t_o)v'(t_o)}x + \frac{-u'(t_o)}{v(t_o)u'(t_o) - u(t_o)v'(t_o)}y + 1 = 0.$$

From 1, the pole of this line is

$$\left(\frac{v'(t_o)}{v(t_o)u'(t_o) - u(t_o)v'(t_o)}, \frac{-u'(t_o)}{v(t_o)u'(t_o) - u(t_o)v'(t_o)}\right).$$

The above holds true for every point $(u(t_o), v(t_o))$. Thus, we can generalize and say that $C^*$ has parametric equations

$$\left(\frac{v'(t)}{u'(t)v(t) - v'(t)u(t)}, \frac{-u'(t)}{u'(t)v(t) - v'(t)u(t)}\right).$$

□

We will now state another realization of duality, using tangents to the curve. This will be a formulation of the concept of duality for projective plane curves. The *real projective plane*, denoted by $\mathbb{RP}^2$, is defined as the plane $\mathbb{R}^2$ along with additional points at infinity that represent intersections of parallel lines. We can also define $\mathbb{RP}^2$ using sets of equivalence classes of nonzero points in $\mathbb{R}^3$. Generally, a point in the real projective space is denoted as $(x : y : z)$, the equivalence class of all points $(\lambda x, \lambda y, \lambda z)$ in $\mathbb{R}^3$, where $\lambda \neq 0$ and $a, b$, and $c$ are not all 0. For each equivalence class $(a : b : c)$ where $c \neq 0$, the point $(x, y, 1) \in \mathbb{R}^3$ can be taken to create the plane $R^2$ as the plane $z = 1$. Each equivalence class $(a : b : 0)$ will then correspond to the point where the line $ay = bx$ in $\mathbb{R}^2$ and all the lines parallel to it intersect. In the same way that points in $\mathbb{RP}^2$ are lines in $\mathbb{R}^3$, lines in $\mathbb{RP}^2$ are planes in $\mathbb{R}^3$. These planes are

sets of equivalence classes $(x : y : z)$ that satisfy the equation $ax + by + c = 0$ for some $a, b$, and $c$ that are not all 0. The planes themselves create a projective space that is called the *dual projective space*, denoted by $\mathbb{RP}^{2*}$. We can now define duality for projective plane curves:

**Definition 3.6.** [5] Let $C$ be the curve in $\mathbb{RP}^2$ given by the homogeneous equation $f(x, y, z) = 0$. Then the dual curve $C^*$ is given by the set of points $\left(\frac{\partial f}{\partial x}(a, b, c) : \frac{\partial f}{\partial y}(a, b, c) : \frac{\partial f}{\partial z}(a, b, c)\right)$ in $\mathbb{RP}^{2*}$ for every point $(a : b : c)$ of $C$.

*Remark.* The notion of duality respects the fact that any real curve on a plane defines a projective curve and vice versa.

We continue our discussion of duality by stating a fundamental theorem:

**Theorem 3.7.** *The dual of a dual curve is the original curve. That is, for any algebraic curve $C$, $(C^*)^* = C$.*

This theorem can be proved using the definition of duality (Definition 3.4), or in cases where $C$ and thus $C^*$ are rational, the algebraic realization of duality (Proposition 3.5). The proof in the former way can be found in [5] and [16]. The proof in the latter way can be seen by performing a computation using

$$(u_1(t), v_1(t)) = \left(\frac{v'(t)}{u'(t)v(t) - v'(t)u(t)}, \frac{-u'(t)}{u'(t)v(t) - v'(t)u(t)}\right),$$

to show that

$$\left(\frac{v_1'(t)}{u_1'(t)v_1(t) - v_1'(t)u_1(t)}, \frac{-u_1'(t)}{u_1'(t)v_1(t) - v_1'(t)u_1(t)}\right) = (u(t), v(t)).$$

Now, we are ready to examine some key properties of an algebraic curve and its dual. We will start by defining some potential singularities of an algebraic curve. We are considering two specific ones, namely cusps and nodes. A *cusp* is defined as a point at which two branches of a curve meet such that the tangents of each branch converge to the same tangent (see Figure 10a for an example of a curve with a cusp). An *node* (also known as an *ordinary double point*) of a plane curve is defined as a point where a curve intersects itself such that two branches of the curve have distinct tangent lines (see Figure 10b for an example of a curve with a node). Ordinary double points can also be isolated. See [7] for further elaboration on these singularities.

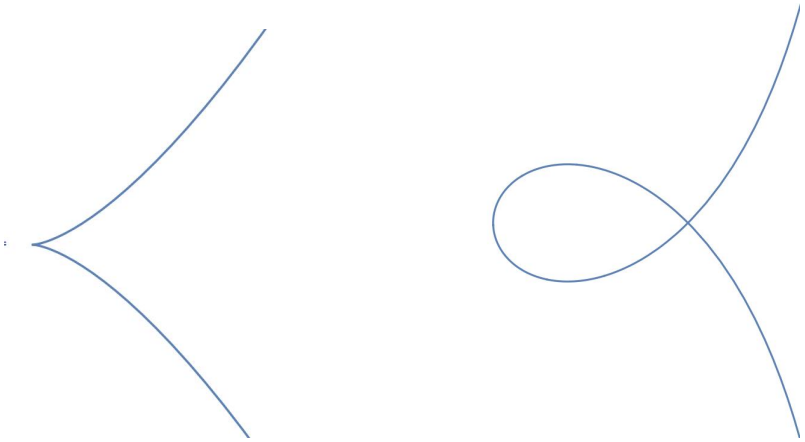

(a) An Example of a Curve With a Cusp

(b) An Example of a Curve With a Node

Figure 10: Singularities of Algebraic Curves

Using these singularities, we are able to articulate a theorem concerning the degree of a dual curve:

**Theorem 3.8.** (Plucker's Formula) *Let $C$ be an algebraic curve with only ordinary double points and simple cusps as singularities such that its dual $C^*$ also only has these types of singularities. Then, if $C$ has degree $d$, the degree $d'$ of $C^*$ is given by*

$$d' = d(d-1) - 2\delta - 3\kappa,$$

*where $\delta$ is the number of ordinary double points of $C$ and $\kappa$ is the number of cusps of $C$.*

*Remark.* If $C$ has higher order singularities, they are considered as multiple double points according to an analysis of the nature of the singularities. For example, an ordinary triple point is considered to be 3 double points.

We are now equipped with enough knowledge of the concept of curve duality to continue our discussion of the properties of the frozen boundary. Curve duality will also play a role in the computations in this paper.

## 3.3 Properties 3 and 4

Let us first state a theorem, proven in the paper by Kenyon and Okounkov [12], that articulates Properties 3 and 4:

**Theorem 3.9.** *Let the boundary contour $\Omega$ be feasible (i.e. a limit of tilable contours), connected, and polygonal with $3d$ sides in coordinate directions (cyclically repeated). Then the frozen boundary $\mathcal{R}$ is a unique, inscribed, rational curve, and its dual is a winding curve of degree $d$.*

Property 3 is explained by the idea of curve duality alone. Property 4, however, requires an additional definition (as stated and further explained in [12]):

**Definition 3.10.** A degree $d$ real algebraic curve $\mathcal{Q}$ is called winding if

1. it intersects any line $L \subset \mathbb{RP}^1$ in at least $d-2$ points counting multiplicity, and
2. there exists a point $p_0 \in \mathbb{RP}^1 \setminus \mathcal{Q}$ called a center, such that any line through $p_0$ intersects $\mathcal{Q}$ in $d$ points.

A useful proposition concerning winding curves is as follows:

**Proposition 3.11.** *All singularities of a winding curve $\mathcal{Q}$ are real. Every branch of $\mathcal{Q}$ through a singularity is real, smooth, and has contact of order $\leq 3$ with its tangent. That is, it has at most ordinary flexes. The only double tangents of a winding curve are ordinary tacnodes (i.e. double cusps) with two branches on the opposite sides of the common tangent.*

The proof of this proposition can be found in [7]. We will now proceed to discussions of computations with hexagonal and octagonal domains.

# 4 Computations of Frozen Boundaries with Hexagonal and Octagonal Domains

## 4.1 Hexagonal Domain: Elliptical Frozen Boundary

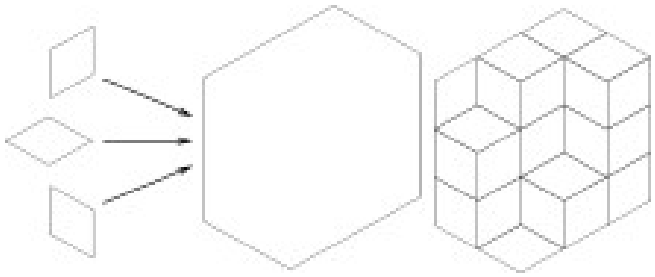

Figure 11: Simple Tiling of a Hexagon [4]

Figure 11, repeated from Section 1, shows a simple rhombus tiling of a hexagon.

We will first define the set $H$ of all hexagons that we will consider. Let $H$ consist of all hexagons that have

1. 3 pairs of equal, parallel sides,
2. all angle measures of $120^o$,
3. and edge lengths such that the quotient of any two is rational.

We will now prove the following:

**Proposition 4.1.** *All hexagons of $H$ are tilable.*

*Proof.* Figure 12 shows how we can create a tilable hexagon satisfying the first two conditions in the theorem and with edge lengths $i, j$, and $k$ for any $i, j, k \in \mathbb{N}$.

[4] This picture is borrowed from [6]

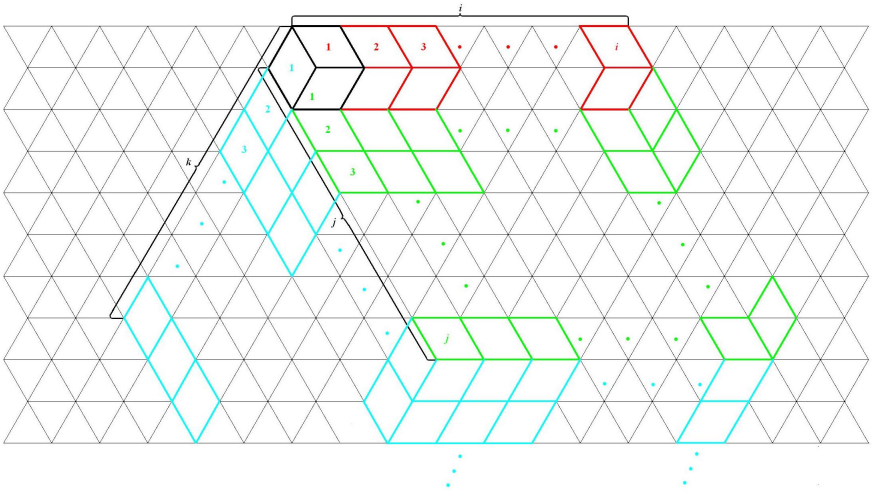

Figure 12: Construction of a Hexagon with Edge Lengths $i, j, k \in \mathbb{N}$

We will now deal with the third condition.

Let us consider any two edge lengths $a, b \in \mathbb{R}$ of a hexagon that satisfies the first two conditions, where $a, b > 0$. Consider a rhombus tiling of the hexagon. Because the tiling must completely cover the hexagonal domain, each edge must be completely covered by equal edges of rhombi. Thus, since all rhombi in a tiling are equal in size, $\frac{a}{m} = \frac{b}{n}$, where $m$ and $n$ are the number of rhombus edges covering edges with lengths $a$ and $b$, respectively. Furthermore, $m, n \in \mathbb{N} \Rightarrow \frac{m}{n} \in \mathbb{Q}$, resulting from the simple fact any number of rhombus tiles must be countable. Hence, we have $\frac{a}{b} = \frac{m}{n}$, indicating that $\frac{a}{b} \in \mathbb{Q}$.

We have thus proven in the last paragraph that any tilable hexagon must have edge lengths such that the quotient of any two is rational (the proof applies to any tilable domain, in fact!). As long as this is true, we can have any positive real edge lengths, for we can scale the hexagon so that the edge lengths are all natural numbers. Since we already proved that such a hexagon is tilable, we can then scale the tile size back with the original domain to construct a tiling of the original domain. In order to prove that the hexagon, along with any other domain, is scalable in such a way, we will consider any $x$-gonal domain $\Omega$ with edge lengths such that the quotient of any two is rational.

Choose any side of length $s_0$ of $\Omega$. For each $i \in \mathbb{N}$ and $i < x$, let $m_i, n_i \in \mathbb{N}$, and let $s_i$ be the length of a distinct side of $\Omega$ so that $\frac{s_i}{s_0} = \frac{m_i}{n_i}$. Let the scale factor for $\Omega$ be $r = \frac{1}{s_0} \prod_{j=1}^{x-1} n_j$. This way, $s_0 r = \prod_{j=1}^{x-1} n_j$ and $s_i r = \left(s_0 \frac{m_i}{n_i}\right) r = m_i \prod_{j \neq i} n_j$, so $s_i r \in \mathbb{N}$ for all sides of $\Omega$.

We have thus proven that any hexagon that satisfies all 3 conditions of the theorem is tilable. □

We can now discuss the computation of the frozen boundary contained in any hexagon of $H$. Let us first determine the nature of the inscribed curve $C$

that is the frozen boundary and that of its dual. By Theorem 3.9, the degree of $C^*$ is 2, which means that the dual curve is a conic. A conic does not have any singularities. Thus, by Plucker's Formula (Theorem 3.8), the degree of $(C^*)^* = C$, is also 2. This means that $C$ is also a conic. By using this fact and looking at a computer simulation with very small rhombi below (Figure 13), we can see that the frozen boundary is an ellipse.

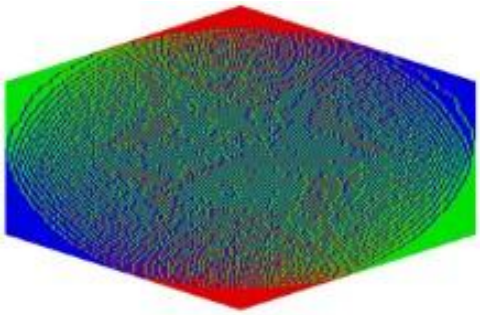

Figure 13: Frozen Boundary in a Hexagon [5]

Now we will proceed with the algorithm for the computation, assuming that we already have the equations of each side of the hexagon. We will first outline each step in the algorithm and then explain each step in detail.

**Algorithm for the Computation**

1. Determine the coordinates of the poles to each of the sides of the hexagon.
2. Solve for the equation of the conic $C^*$ that contains all of the poles. This is the dual conic to the inscribed conic because of Definition 3.4.
3. Compute the equation of the dual of conic $C^*$. This will be the inscribed conic $C$ by Theorem 3.7.

Using Equation 1 from Proposition 3.5, we can execute step 1 in the algorithm. To avoid complications in this step, let us position the hexagon so none of the edges pass through the origin.

In order to execute step 2, we use the general equation of a conic:

$$ax^2 + by^2 + cz^2 + dxy + exz + fyz = 0.$$

To make this a conic in the $xy$ plane, we will set $z = 1$ (the intersection of the conic with the plane $z = 1$. Thus, we will have

$$ax^2 + by^2 + c + dxy + ex + fy = 0.$$

[5] This picture is borrowed from [6]

If we divide this equation by $a$, we will only have 5 coefficients for which to solve. Therefore, we only need poles of 5 sides of the hexagon in order to make a system of linear equations that will solve for the 5 coefficients. Because the frozen boundary is unique, there will be exactly one solution for the coefficients.

For step 3, we need a formula for the dual of a conic. Before we state this, let us introduce the quadratic form of the conic $ax^2+by^2+cz^2+dxy+exz+fyz=0$:

$$\begin{pmatrix} x & y & z \end{pmatrix} \begin{pmatrix} a & d/2 & e/2 \\ d/2 & b & f/2 \\ e/2 & f/2 & c \end{pmatrix} \begin{pmatrix} x \\ y \\ z \end{pmatrix} = 0.$$

As shown above, every conic can be represented in this way. Now, we can make a proposition stating the quadratic form of a dual of a conic.

**Proposition 4.2.** *Let $C$ be the conic* $\begin{pmatrix} x & y & z \end{pmatrix} \begin{pmatrix} a & d & e \\ d & b & f \\ e & f & c \end{pmatrix} \begin{pmatrix} x \\ y \\ z \end{pmatrix} = 0$ (or $ax^2+by^2+cz^2+2dxy+2exz+2fyz=0$). *Then $C^*$ is the conic* $\begin{pmatrix} x & y & z \end{pmatrix} \begin{pmatrix} a & d & e \\ d & b & f \\ e & f & c \end{pmatrix}^{-1} \begin{pmatrix} x \\ y \\ z \end{pmatrix} = 0.$

*Proof.* To prove this, we will use the gradients realization of duality (Proposition 3.6), since the conic $C$ can be represented by the homogeneous equation $f(x,y,z)=0$ in the real projective space. Let $(p:q:r)$ be a point in $\mathbb{RP}^2$ on this conic. We are looking for the corresponding point $(x:y:z)=\left(\frac{\partial f}{\partial x}(p,q,r) : \frac{\partial f}{\partial y}(p,q,r) : \frac{\partial f}{\partial z}(p,q,r)\right)$. Since the gradient vector is perpendicular to the surface tangent to $C$ at $(p,q,r)$, and because $(p:q:r)$ is part of this surface, $\langle p,q,r\rangle \cdot \langle x,y,z\rangle = px+qy+rz=0$. Based on the quadratic form for $C$, $\begin{pmatrix} p & q & r \end{pmatrix} \begin{pmatrix} a & d & e \\ d & b & f \\ e & f & c \end{pmatrix} \begin{pmatrix} p \\ q \\ r \end{pmatrix} = 0$. If we let $\begin{pmatrix} a & d & e \\ d & b & f \\ e & f & c \end{pmatrix} \begin{pmatrix} p \\ q \\ r \end{pmatrix} = \begin{pmatrix} x' \\ y' \\ z' \end{pmatrix}$, we see that $\begin{pmatrix} p & q & r \end{pmatrix} \begin{pmatrix} x' \\ y' \\ z' \end{pmatrix} = px'+qy'+rz' = 0$.

Hence, $\langle p,q,r\rangle \cdot \langle x',y',z'\rangle = 0$, so both $\langle x',y',z'\rangle$ and $\langle x,y,z\rangle$ are perpendicular to $\langle p,q,r\rangle$, meaning that $(x':y':z')=(x:y:z)$. Hence, $\begin{pmatrix} a & d & e \\ d & b & f \\ e & f & c \end{pmatrix} \begin{pmatrix} p \\ q \\ r \end{pmatrix} = \begin{pmatrix} x \\ y \\ z \end{pmatrix}$ under the equivalence classes of $\mathbb{RP}^2$. We can also see this if we calculate the gradient $(x:y:z) = \left(\frac{\partial f}{\partial x}(p,q,r) : \frac{\partial f}{\partial y}(p,q,r) : \frac{\partial f}{\partial z}(p,q,r)\right) = (2ap+2dq+2er : 2bq+dp+fr : 2cr+ep+fq) \Rightarrow 2 \begin{pmatrix} a & d & e \\ d & b & f \\ e & f & c \end{pmatrix} \begin{pmatrix} p \\ q \\ r \end{pmatrix} =$

$\begin{pmatrix} x \\ y \\ z \end{pmatrix}$ under the equivalence classes of $\mathbb{RP}^2$. If we divide by 2, we are still in the equivalence class represented by $(x : y : z)$, reinforcing the previous result. Now, we can manipulate this result to obtain the quadratic form for $C^*$:

$$\begin{pmatrix} a & d & e \\ d & b & f \\ e & f & c \end{pmatrix} \begin{pmatrix} p \\ q \\ r \end{pmatrix} = \begin{pmatrix} x \\ y \\ z \end{pmatrix} \Rightarrow \begin{pmatrix} p \\ q \\ r \end{pmatrix} = \begin{pmatrix} a & d & e \\ d & b & f \\ e & f & c \end{pmatrix}^{-1} \begin{pmatrix} x \\ y \\ z \end{pmatrix} \Rightarrow$$

$$\begin{pmatrix} x & y & z \end{pmatrix} \begin{pmatrix} a & d & e \\ d & b & f \\ e & f & c \end{pmatrix}^{-1} \begin{pmatrix} x \\ y \\ z \end{pmatrix} = \begin{pmatrix} x & y & z \end{pmatrix} \begin{pmatrix} p \\ q \\ r \end{pmatrix} = xp + yq + zr = 0.$$

Hence, for every point $(p : q : r) \in C$, the point $(x : y : z) \in C^*$ will satisfy the equation:

$$\begin{pmatrix} x & y & z \end{pmatrix} \begin{pmatrix} a & d & e \\ d & b & f \\ e & f & c \end{pmatrix}^{-1} \begin{pmatrix} x \\ y \\ z \end{pmatrix} = 0.$$

□

We now have the algorithm for the explicit computation of the frozen boundary with our special type of hexagonal domains. Figures 14, 15, and 16 show some examples of the results obtained from the implementation of this algorithm. Although these examples may not have rational quotients for any two sides, they are very close (infinitely close) approximations of tilable domains and their frozen boundaries. This is so because we can make infinitely close rational approximations of irrational numbers, and slightly adjust the edges of a domain to fit these rational approximations. (Side note: because we did not use the fact that the hexagon has to be tilable in the algorithm, it will yield the inscribed curve for any hexagon that has a conic for this inscribed curve.)

- Equations of Sides
  - $y = -\sqrt{3}(x - 3)$
  - $y = \sqrt{3}(x - 3)$
  - $y = -\sqrt{3}(x + 3)$
  - $y = \sqrt{3}(x + 3)$
  - $y = -2$
  - $y = 2$
- Equation of Frozen Boundary
  - $x^2 + 1.9166667y^2 - 7.66667 = 0$

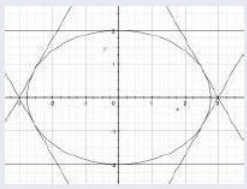

Frozen Boundary in the Hexagonal Domain

Figure 14: Hexagonal Example 1

- Equations of Sides
  - $y = 0.5x + 2.5$
  - $y = 0.5x - 2.5$
  - $y = 16.66(x + 2)$
  - $y = 16.66(x - 2)$
  - $y = -.66(x + 2)$
  - $y = -.66(x - 2)$
- Equation of Frozen Boundary
  - $-0.22254026037x^2 - 0.268822y^2 + 0.465063686975 - 0.32382566942xy = 0$

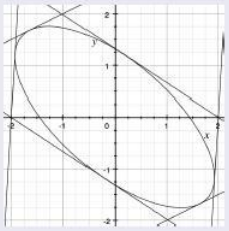

Frozen Boundary in the Hexagonal Domain

Figure 15: Hexagonal Example 2

- Equations of Sides
  - $y = x - 1$
  - $y = x - 3$
  - $y = -.26795x - 1$
  - $y = -.26795x + 1$
  - $y = -3.73205(x - .25)$
  - $y = -3.73205(x - 2.6782)$
- Equation of Frozen Boundary
  - $-0.404941711057x^2 - 0.7087299025y^2 - 1.110655775625 + 0.5188288546999998xy + 1.4967493790500002x - 1.4174623775y = 0$

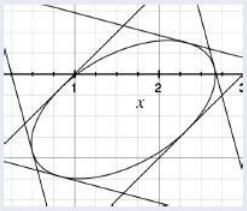

Frozen Boundary in the Hexagonal Domain

Figure 16: Hexagonal Example 3

## 4.2 Octagonal Domain: Cardioidal Frozen Boundary

Recall from the previous subsection the definition of the set $H$ of all the hexagons considered in our computations. The set $O$ of octagons that we will consider will be derived from a special subset $H_S$ of $H$, defined so that $H_S$ consists of all hexagons in $H$ that have at most 2 distinct side lengths (i. e. at least 2 pairs of equal, parallel sides will consist of the same side length). Let us consider a hexagon $H_{m,n} \in H_S$, with 2 sides of length $m$ and 4 sides of length $n$ ($m = n$ is a possibility). Choose $l$ such that $0 < l < n$ and $\frac{l}{n} \in \mathbb{Q}$. Now position a $60^o$

rhombus with side length $l$ inside $H_{m,n}$ so that each of 2 adjacent edges of the rhombus lies on each of two adjacent sides of length $n$. Remove the area covered by the rhombus to obtain an octagon. See Figure 17 (repeated from Section 1) for a visual representation of this construction.

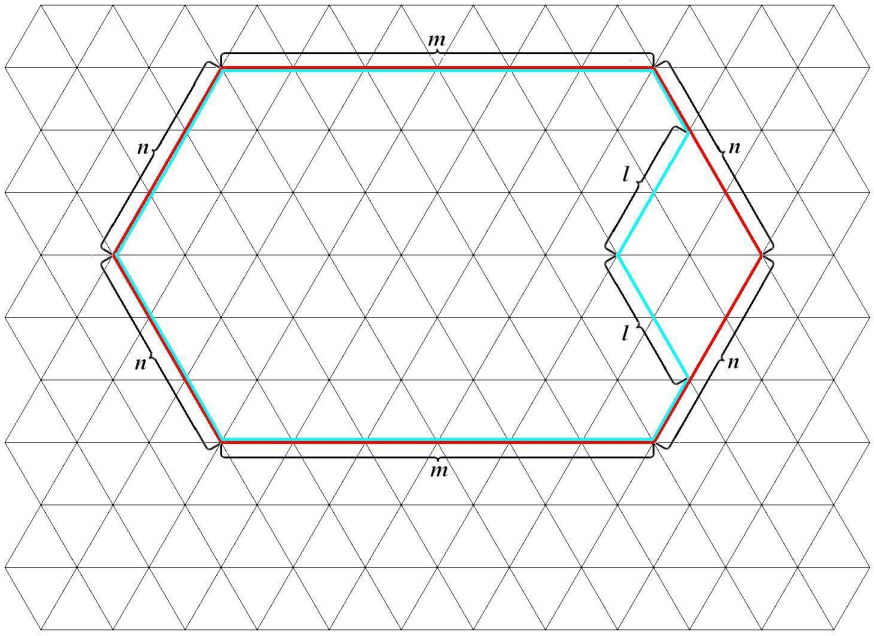


Figure 17: A Construction of a Considered Octagon from a Considered Hexagon

$O$ is defined as the set of all possible octagons constructed using all $H_{i,j} \in H_S$ and all $k$ for each hexagon $H_{i,j}$ such that $0 < k < j$ and $\frac{k}{j} \in \mathbb{Q}$.

We will now show that all octagons in $O$ are tilable.

The first step is to illustrate how we can tile a rhombus with smaller rhombi so that one side of the original rhombus is covered with any number of smaller tiles. Figure 18 shows how we can add tile extensions on to a rhombus until we reach the desire number of tiles, constructing a larger rhombus (this is analogous to tiling a square with smaller squares. In fact, [2] discusses an affine modification of lozenge that will transform one type of lozenge into a square). We can then scale the whole tiling of the larger rhombus to any size.

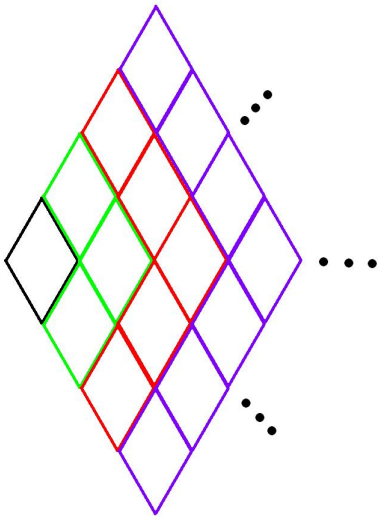

Figure 18: A Tiling of a Rhombus with Smaller Rhombus Tiles

We will now further consider the construction pictured in Figure 17. Let us first scale the domain so that all edge lengths, including those of the octagon, are natural numbers. Let us denote this new edge lengths as $l', m'$, and $n'$. As proven in the previous subsection, this can be done since any two lengths $l, m$, and $n$ have a rational quotient, which indicates that an edge with length $n - l$ and any other edge of the octagon also have a rational quotient.

Figure 19 shows how we can divide the domain into tilable parts (the part boundaries are outlined in yellow) with tile edge length 1. The rhombus with side lengths $l'$ will be completely tiled, as proven with Figure 18. This indicates that we can remove this rhombus and leave the remaining tiles intact, demonstrating how the constructed octagonal domain will be tilable. We can then scale back to the original domain. Since this whole process can be done with any octagon of $O$, we have shown that all octagons in $O$ are tilable.

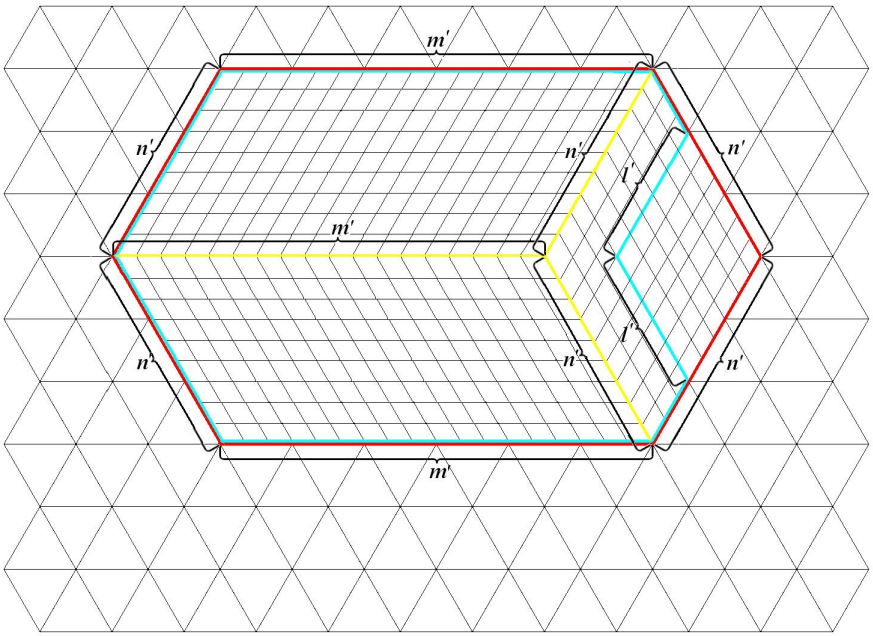


Figure 19: Tilability of a Scaled Octagonal Domain

We will now discuss how to compute the frozen boundary contained in any octagon of $O$. Figure 20 shows an image of a considered octagonal domain and the frozen boundary it contains. The image illustrates how the frozen boundary is a cardioid. In fact, this is not necessarily a perfect cardioid, but rather a compressed or elongated one. By Theorem 3.9 (considering an extra degenerate edge of the domain), the dual of this cardioid has degree 3. In order to create symmetry to simplify the computations, we will translate the domain so that the cusp of the cardioid is on the $x$-axis and so that the domain is symmetric about the $x$-axis.

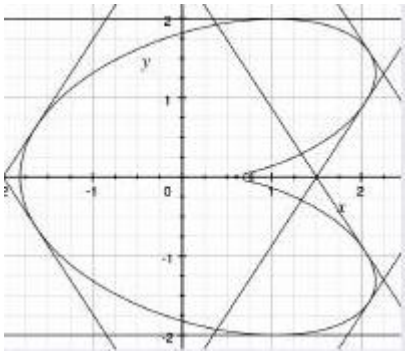


Figure 20: The Frozen Boundary in an Octagon

Now, we will use the same algorithm as in the previous subsection to perform the computation:

**Algorithm for the Computation**

1. Determine the coordinates of the poles to each of the sides of the octagon.
2. Solve for the equation of the cubic curve $C^*$ that contains all of the poles. This is the dual cubic to the inscribed cardioid because of Definition 3.4.
3. Compute the equation of the dual of cubic $C^*$. Again, this will be the inscribed cardioid $C$ by Theorem 3.7.

Using Equation 1 from Proposition 3.5, we can again execute step 1 in the algorithm. To avoid complications in this step, let us again position the octagon so that none of the edges pass through the origin.

Step 2 requires us to determine the general equation of the cubic we're interested in. Since we have made it so it is symmetric about the $x$-axis, we can eliminate all terms with an odd degree of $y$. Hence, we have:

$$ax^3 + bxy^2 + cy^2 + dx^2 + ex + f = 0.$$

If we divide by $a$, we will have 5 coefficients for which to solve. However, we only have 4 linear equations, since each side of the octagon has a corresponding side that is just its symmetric side about the $x$-axis, which will not give another equation. However, if we use the fact the double tangent of the cardioid corresponds to a node of the cubic on the $x$-axis, we will see that there is a double root when $y = 0$. Hence, if $r$ is the double root and $s$ is the single root when $y = 0$, we have:

$$(x - r)^2(x - s) = x^3 - sx^2 - 2rx^2 + 2rsx + r^2x - r^2s = 0.$$

Thus, we can create the following equation:

$$x^3 + bxy^2 + cy^2 - (s + 2r)x^2 + (r^2 + 2rs)x - r^2s = 0.$$

Now, we have 4 equations and 4 unknowns for which to solve. Although these equations are not linear, Wolfram Mathematica will be able to solve them.

For step 3, we will use Proposition 3.5 to find the equation of the dual curve that is the frozen boundary in parametric form. First, we will have to convert the cubic into parametric form. We know this can be done because of Property 2. Proposition 3.5 indicates that the dual curve is also rationally parameterizable. An algorithm for this (using the double point of the cubic) can be found on page 116 (Chapter 4) of [20]. If we wish to convert this dual to cartesian coordinates, we can use an algorithm on page 109 (Chapter 4) of [20].

Thus, we can compute the frozen boundary of rhombus tilings of this octagon using these steps. Figure 21 shows an example of a result with this domain. As with hexagonal domains in the previous subsection, this example is a very close approximation of a tilable domain and the frozen boundary associated with it.

- Equations of Sides
- $y = -\sqrt{3}(x+2)$
- $y = \sqrt{3}(x+2)$
- $y = -\sqrt{3}(x-3)$
- $y = \sqrt{3}(x-3)$
- $y = -\sqrt{3}(x-1.5)$
- $y = \sqrt{3}(x-1.5)$
- $y = -2$
- $y = 2$
- Equation of Frozen Boundary
  - $-819.68 + 5255.08x - 10097.5x^2 + 2939.42x^3 + 5654.49x^4 - 126470y^2 - 47651.6xy^2 + 20749x^2y^2 + 38224.3y^4 = 0$

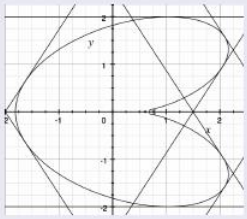

Frozen Boundary in the Octagonal Domain

Figure 21: An Example of the Frozen Boundary in an Octagon

# 5 A Frozen Boundary that is a 3-tangent Curve

In the last section, we had an example of a frozen boundary that had a double tangent. In this section, we will examine a set $\Omega_3$ of special, geometrically similar domains that contain frozen boundaries that are 3-tangent curves. One example of a domain $\Omega_3' \in \Omega_3$ is pictured below (Figure 22). This superimposition of $\Omega_3'$ on a triangular lattice allows us to see that it is indeed tilable (one of its tilings is outlined). $\Omega_3$ will consist of all domains that are geometrically similar to $\Omega_3'$. All of these domains will also be tilable, since we can proportionally increase or decrease tile size.

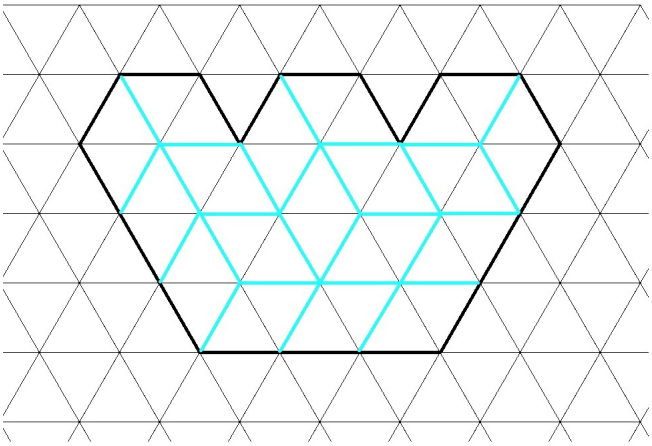

Figure 22: An Example of a Domain $\Omega_3' \in \Omega_3$

Now that we have our set of tilable domains, we can begin our discussion of how to explicitly compute the frozen boundaries associated with them. Figure 23 shows a result with one example of a tilable domain.

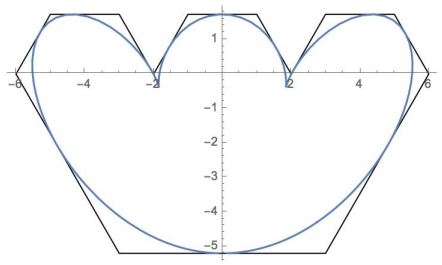


Figure 23: A Result with a 3-tangent Frozen Boundary in a Domain of $\Omega_3$

We will consider any domain that is in our set of tilable ones. By Property 3, the dual curve $Q$ to the inscribed one has degree 4 since our domain has 12 sides. From this information alone we will have $\sum_{n=1}^{5} n = 15$ terms and thus 15 coefficients for which to solve. Now, we will try to eliminate as many more unknown coefficients as possible.

First, we translate the domain so that it is symmetric with respect to the $y$-axis, creating this same symmetry in the frozen boundary and thus the dual of the frozen boundary as well (by Definitions 3.4 and 3.3). This eliminates all terms with odd degrees in x, leaving us with 9 terms of $Q$. Let us now examine what occurs in $Q$ when $x = 0$ (when we have a polynomial in only one variable $y$). The points of $Q$ at $x = 0$ will correspond to tangents of the frozen boundary perpendicular to the $y$-axis, by Definitions 3.4 and 3.3. From Figures 22 and 23, we can see that we have one triple tangent and one single tangent to the frozen boundary perpendicular to the $y$-axis. Thus, we know that we have in $Q$ at $x = 0$ a triple point that corresponds to the triple tangent and a single point that corresponds to the single tangent. We can now set up our equation for $Q$ as follows:

$$Q(x, y) = a(y - p_t)^3(y - p_s) + by^2x^2 + cyx^2 + dx^2 + ex^4 = 0,$$

where $p_t$ is the $y$-coordinate of the triple point at x=0, $p_s$ is the $y$-coordinate of the single point at x=0, and $a, b, c, d$, and $e$ are the unknown coefficients that we will solve for. Notice how we eliminated 4 unknown coefficients by representing coefficients of terms with degree 0 in $x$ using 1 unknown ($a$) instead of 5. We can in fact divide by this $a$, since $Q(x, y) = 0$, to eliminate one unknown coefficient. We can then represent $Q(x, y)$ as

$$Q(x, y) = (y - p_t)^3(y - p_s) + ay^2x^2 + byx^2 + cx^2 + dx^4 = 0.$$

Even though we have already used the edges perpendicular to the $y$-axis, we still have 4 nonsymmetric edges of our domain to obtain 4 points of $Q$ that

will allow us to set up a system of linear equations to solve for $a, b, c$, and $d$ (see Figure Domain 22). However, we can also use the fact that we can rationally parametrize $Q$ with lines of slope t passing through the triple point, since there is at most one other point of intersection with $Q$ (Fundamental Theorem of Algebra). This algorithm (also used in previous cardioid computations) is explained further on page 116 (Chapter 4) of [20].

Based on this algorithm, we can translate $Q(x, y)$ so that the triple point is at the origin and have lines of the form $y = tx$ passing through the triple point. Then, since the point $(0, 0)$ is a triple point, we will be able to factor out $x^3$ from $Q(x, y)$. Thus, the translated $Q(x, y)$ will have terms of degree no less than 3. Let us now work with these facts:

$$Q(x, y + p_t) = y^3(y + p_t - p_s) + a(y + p_t)^2x^2 + b(y + p_t)x^2 + cx^2 + dx^4 = 0.$$

$$Q(x, tx + p_t) = (tx)^3(tx + p_t - p_s) + a(tx + p_t)^2x^2 + b(tx + p_t)x^2 + cx^2 + dx^4 = 0.$$

From this, we will have three terms with degree in $x$ less than 3: $ap_t^2x^2$, $bp_tx^2$ and $cx^2$. We thus have

$$ap_t^2x^2 + bp_tx^2 + cx^2 = 0 \Rightarrow c = -(ap_t^2 + bp_t), \tag{2}$$

eliminating yet another unknown coefficient and yielding a new form for our equation of $Q(x, y)$:

$$Q(x, y) = (y - p_t)^3(y - p_s) + ay^2x^2 + byx^2 - (ap_t^2 + bp_t)x^2 + cx^4 = 0.$$

We can now safely choose any three of the four nonsymmetric edges of our domain to obtain 3 points of $Q$ that will allow us to set up a system of linear equations to solve for $a, b$, and $c$, simplifying the final computation. We can then use the fourth point of $Q$, obtained from the fourth nonsymmetric edge of the domain, to verify that we do indeed have the correct equation of $Q(x, y) = 0$ after solving the system of linear equations in three variables.

We now have our equation of the dual curve to the frozen boundary in cartesian coordinates. Using the aforementioned parametrization technique as well as Proposition 3.5, we can compute the dual curve of $Q$ to obtain the desired equation of the frozen boundary in parametric form.

# 6 Generalization to an $n$-tangent Curve

This section will be devoted to generalizing the results in the previous section. As an intermediate, however, we will first elaborate on the method for obtaining results with a frozen boundary that is the 4-tangent curve. In many ways, the discussions in this section are logical extensions of the discussions in the previous one.

## 6.1 A Frozen Boundary that is a 4-tangent Curve

Let us first begin this subsection by showcasing a visual result of the computations for this frozen boundary (Figure 24):

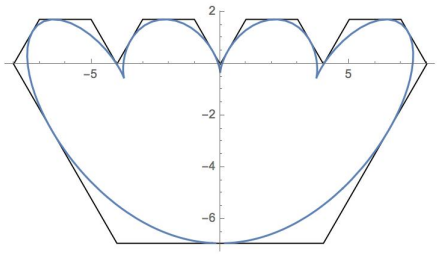


Figure 24: A Result with a 4-tangent Frozen Boundary in a Domain of $\Omega_4$

We will first examine the superimposition of one example of a considered domain $\Omega_4' \in \Omega_4$ (where $\Omega_4$ is the set of considered tilable domains) on a triangular lattice to reinforce the fact that it is tilable (see Figure 25). Notice that this is just a domain from the last section with one addition (see Figure 26). The domains in $\Omega_4$ will be all domains that are geometrically similar to $\Omega_4'$. Now, we can begin our discussion of how to explicitly compute the frozen boundary for any domain of $\Omega_4$.

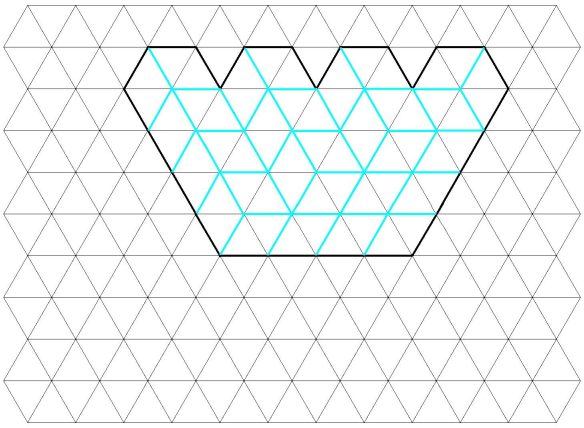

Figure 25: Tilability of $\Omega_4'$

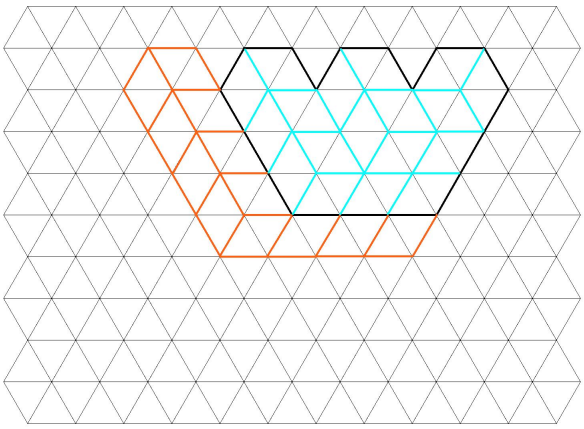

Figure 26: Construction of $\Omega'_4$ from $\Omega'_3$

By Property 3, the dual curve $Q$ to the inscribed one has degree 5 since our domain has 15 sides. From this information alone we will have $\sum_{n=1}^{6} n = 21$ terms and thus 21 coefficients for which to solve. Again, we will try to eliminate as many more unknown coefficients as possible.

We still translate the domain so that it is symmetric with respect to the $y$-axis, creating this same symmetry in the frozen boundary and thus the dual of the frozen boundary as well (by Definitions 3.4 and 3.3). This eliminates all terms with odd degrees in x, leaving us with 12 terms of $Q$. When we set $x = 0$, the points of $Q$ will correspond to tangents of the frozen boundary perpendicular to the $y$-axis, by Definitions 3.4 and 3.3. From Figures 24 and 25, we can see that we have one quadruple tangent and one single tangent to the frozen boundary perpendicular to the $y$-axis. Thus, we know that we have in $Q$ at $x = 0$ a quadruple point that corresponds to the quadruple tangent and a single point that corresponds to the single tangent. We can now set up our equation for $Q$ as follows:

$$Q(x, y) = (y - p_q)^4(y - p_s) + ay^3x^2 + by^2x^2 + cyx^2 + dx^2 + eyx^4 + fx^4 = 0,$$

where $p_q$ is the $y$-coordinate of the quadruple point at x=0, $p_s$ is the $y$-coordinate of the single point at x=0, and $a, b, c, d, e$ and $f$ are the unknown coefficients that we will solve for. Notice how we eliminated 5 unknown coefficients by representing coefficients of terms with degree 0 in $x$ using 1 unknown instead of 6 (We have also already divided by this unknown).

With the 3-tangent curve, we had sufficient nonsymmetric edges to set up a system of linear equations. With this case, however, we only have 5 non-symmetric edges but 6 unknown coefficients (we have already used the edges perpendicular to the $y$-axis). It thus becomes necessary rather than convenient to use the fact that we can rationally parametrize $Q$ with lines of slope t passing through the quadruple point. This is still the same algorithm further explained on page 116 (Chapter 4) of [20].

As before, we translate $Q(x, y)$ so that the quadruple point is at the origin and have lines of the form $y = tx$ passing through the quadruple point. Then, since the point $(0, 0)$ is a quadruple point, we will be able to factor out $x^4$ from $Q(x, y)$. Thus, the translated $Q(x, y)$ will have terms of degree no less than 4. Let us now work with these facts:

$$\begin{gathered}Q(x, y + p_q) = y^4(y + p_q - p_s) + a(y + p_q)^3x^2 + b(y + p_q)^2x^2 \\ +c(y + p_q)x^2 + dx^2 + e(y + p_q)x^4 + fx^4 = 0. \\ Q(x, tx + p_q) = (tx)^4(tx + p_q - p_s) + a(tx + p_q)^3x^2 + b(tx + p_q)^2x^2 \\ +c(tx + p_q)x^2 + dx^2 + e(tx + p_q)x^4 + fx^4 = 0.\end{gathered}$$

From this, we will have 7 terms with degree in $x$ less than 4: $3atp_q^2x^3$, $ap_q^3x^2$, $2btp_qx^3$, $bp_q^2x^2$, $ctx^3$, $cp_qx^2$ and $dx^2$. We thus have:

$$\begin{gathered}3atp_q^2x^3 + 2btp_qx^3 + ctx^3 = 0 \Rightarrow c = -(3ap_q^2 + 2bp_q), \text{ and} \\ ap_q^3x^2 + bp_q^2x^2 + cp_qx^2 + dx^2 = 0 \Rightarrow ap_q^3x^2 + bp_q^2x^2 - \\ (3ap_q^2 + 2bp_q)p_qx^2 + dx^2 = 0 \Rightarrow \\ \Rightarrow d = -(ap_q^3 + bp_q^2 - (3ap_q^2 + 2bp_q)p_q) = 2ap_q^3 + bp_q^2\end{gathered} \tag{3}$$

This eliminates the unknown coefficients $c$ and $d$ from our original equation, yielding a new form for our equation of $Q(x, y)$:

$$\begin{gathered}Q(x, y) = (y - p_q)^4(y - p_s) + ay^3x^2 + by^2x^2 \\ -(3ap_q^2 + 2bp_q)yx^2 + (2ap_q^3 + bp_q^2)x^2 + cyx^4 + dx^4 = 0.\end{gathered}$$

We now have four unknown coefficients, so we can choose any 4 of the 5 nonsymmetric (and not perpendicular to the $y$-axis) edges of our domain to obtain 4 points of $Q$ that will allow us to set up a system of linear equations to solve for $a$, $b$, $c$, and $d$. There is, however, another trick we can employ to eliminate one more unknown coefficient and further simplify the computation.

This trick involves translating the domain so that the vertex on the $y$-axis lies at the origin. There will then be two edges of the domain passing through the origin, so we know that the homogenization of $Q$ contains two points (where one is the reflection of the other across the $y$-axis) where z=0 (point at infinity). Let one of these points be $(x_0, y_0, 0)$ (the other will be identical except for a sign change for the $x$-coordinate, but this sign change is irrelevant since we have already eliminated all terms with odd degrees in $x$).

If the homogenization of $Q$ is $Q(x, y, z)$, we have:

$$Q(x_0, y_0, 0) = (y_0)^5 + a(y_0)^3(x_0)^2 + c(y_0)(x_0)^4 = 0 \Rightarrow c = -\left(\left(\frac{y_0}{x_0}\right)^4 + a\left(\frac{y_0}{x_0}\right)^2\right).$$

We know we can divide by $x_0$ because the edges of the domain passing through the origin are not perpendicular to the $y$-axis, indicating that $x_0 \neq 0$

(see Figure 24). This manipulation yields a new form for $Q$, dependent upon only 3 parameters:

$$Q(x,y) = (y-p_q)^4(y-p_s) + ay^3x^2 + by^2x^2 - (3ap_q^2 + 2bp_q)yx^2$$

$$+(2ap_q^3 + bp_q^2)x^2 - \left(\left(\frac{y_0}{x_0}\right)^4 + a\left(\frac{y_0}{x_0}\right)^2\right)yx^4 + cx^4 = 0.$$

We have now simplified our computation so that we can choose any 3 of 4 nonsymmetric edges of the domain (we have already used the edges perpendicular to the $y$-axis and the ones passing through the origin). Using the poles obtained from these edges, we can set up a system of linear equations to solve for $a$, $b$, and $c$. The unused nonsymmetric edge can be used to obtain another point of $Q$ in order to verify that we do indeed have the correct equation of $Q(x,y) = 0$ after solving the system of linear equations in three variables.

We now have our equation of the dual curve to the frozen boundary in cartesian coordinates. Using the aforementioned parametrization technique as well as Proposition 3.5, we can compute the dual curve of $Q$ to obtain the desired equation of the frozen boundary in parametric form.

## 6.2 A Frozen Boundary that is an $n$-tangent Curve

Let $\Omega_n$ ($n \geq 3$) be the set of considered domains with $n$-tangent frozen boundaries. $\Omega_n$ can be defined recursively for various $n$. Figure 27 illustrates how we will create tilable additions (shown in different colors) to reach a tilable domain $\Omega'_n \in \Omega_n$ for any $n > 3$. We will consider $\Omega'_n$ reached when there are $n$ distinct upper segments (edges) of our construction (i. e. the number of additions we have constructed is $n-3$). $\Omega_n$ will consist of all domains geometrically similar to $\Omega'_n$. As seen in Figure 27, we can use induction, where $\Omega'_3$ is the base case and a colored addition creates the inductive step from $\Omega'_n$ to $\Omega'_{n+1}$, to prove that $\Omega'_n$ is tilable for any $n \geq 3$. In fact, if we were to take away an addition away from $\Omega_3$, we would reach $\Omega_2$. Repeating this step would result in $\Omega_1$, which would just be a regular hexagon in the aforementioned set $H$. As with $\Omega_3$, $\Omega_n$ will contain all tilable domains because we can proportionally increase or decrease tile size. Notice that another defining characteristic of any domain in any set $\Omega_n$ is that the sum of the lengths of the distinct upper segments (edges) is equal to the length of the bottom side.

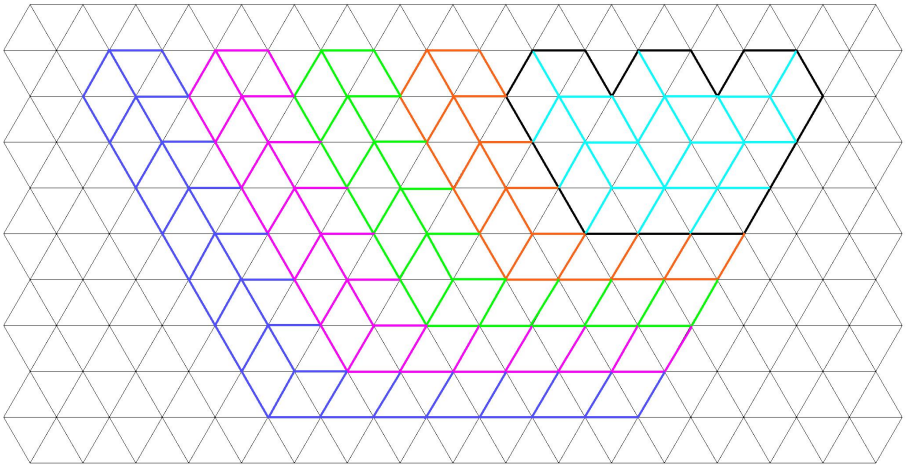

Figure 27: Construction of a Domain $\Omega'_n \in \Omega_n$ from a Domain $\Omega'_3 \in \Omega_3$

Let us now show that we can find an algorithm to compute the frozen boundary contained in any domain of $\Omega_n$. As a start, we can consider domains of $\Omega_2$, since we already have an algorithm for any hexagon of $\Omega_1$.

Any domain $\Omega'_2 \in \Omega_2$ will have 9 edges, meaning that the degree of the dual to the frozen boundary will be 3 (Property 3). This yields $\sum_{n=1}^{4} n = 10$ terms and thus 10 coefficients for which to solve. Translating the domain so that it is symmetric with respect to the $y$-axis eliminates all terms with odd degrees in $x$, leaving us with 6 terms and unknown coefficients. Using the fact that we have a double and single point at $x = 0$, we can use only 1 unknown coefficient rather than 4 to represent coefficients of terms with degree 0 in $x$. Dividing by this 1 unknown coefficient, we will be left with only 2 unknown coefficients for which to solve. We already have 3 nonsymmetric (and not perpendicular to the $y$-axis) edges of $\Omega'_2$ to obtain 3 points of $Q$. We can use 2 of those points to solve for $a$ and $b$, or we can translate $\Omega'_2$ so that the vertex at the $y$-axis lies at the origin, using the homogenization trick explained in the previous subsection. This will allow us to express the coefficients of $Q$ in only 1 unknown. We can then use any 1 of 2 nonsymmetric edges (not perpendicular to the $y$-axis and not passing through the origin) to obtain a point of $Q$ that will allow us to solve for the unknown coefficient. We then use the parametrization technique used with domains in $\Omega_3$ and in $\Omega_4$ as well as Proposition 3.5 to solve for the frozen boundary.

We will move on to any domain $\Omega'_n \in \Omega_n$, for any integer $n > 4$. We know from the previous discussions that adding an addition to $\Omega'_n$ will remove 1 edge and add 4 to $\Omega'_{n+1}$. Thus, the number of edges increases by 3 with each increase in $n$ by 1, indicating that the degree of the dual curve to the frozen boundary will also increase by 1 in degree (Property 3). Thus, for $\Omega'_n$, the degree of the dual curve $Q_n(x, y)$ to the frozen boundary is $n + 1$. We will thus have $\sum_{i=1}^{i+2} i$ unknown coefficients for which to solve.

Let us try to represent $Q_n$ with the minimal amount of unknown coefficients of terms. As we have done before, we can translate the domain so that it is symmetric with respect to the $y$-axis, leaving only terms with even degrees in $x$. We already know that we can represent terms with degree 0 in $x$ as $a(y-p_n)^n(y-p_s)$, where $a$ is a coefficient, $p_n$ is the $n$-fold point on the $y$-axis, and $p_s$ is the single point on the $y$-axis. Since we will have $Q_n = 0$, we can divide by $a$, leaving unknown coefficients only for terms with degrees in $x$ greater than 0 (and still only even).

In order to further reduce the amount of unknown coefficients, we will group our terms so that a term $\kappa(i,j)x^iy^j \in T_i$ (i .e. group together all terms with the same degree in $x$). Here, $\kappa(i,j)$ is a function that yields the coefficient of a term with variables $x^iy^j$. We will now prove the following:

**Proposition 6.1.** *Using the fact that the equation $Q_n = 0$ is rationally parametrizable, we can represent the coefficients of every term of every set $T_i$ using only two unknown ones. Furthermore, in the case where $n+1$ is even, we can represent the coefficients of $T_{n+1}$ using only one unknown, for $\kappa(n+1,0)x^{n+1}$ is the only term of the set.*

*Proof.* We will begin the proof by referring to the previously employed method for eliminating unknown coefficients, using the aforementioned rational parametrization technique (see Sections 5 and 6.1). From this, we know that the polynomial $Q_n(x, tx+p_n)$, when simplified, has no terms with degrees in $x$ less than $n$, for we can factor out $x^n$ due to the $n$-fold point now at the origin. We can use this fact to eliminate coefficients of terms in each set $T_i$ (other than $T_{n+1}$ (if it exists), which will now be excluded from further discussion until stated otherwise, based on the statement of the proposition).

Let us now consider a set $T_i$. For $Q_n(x, tx+p_n)$, each term in $T_i$ will have variables $x^i(tx)^r = t^rx^{i+r}$, for some exponent $r$. As we did in Equations 2 and 3, we can group all terms of $T_i$ with the same exponents for $t$ and $x$, set the sum equal to 0, and eliminate one unknown coefficient for each grouping $G_{i,r}$ (only for terms with degrees $i+r$ in $x$ less than $n$, as discussed in the previous paragraph). Notice how for a different $i$, we will need a different exponent $r$ of $t$ with the same exponent $i+r$ of $x$. Thus, there will indeed be no two terms from different $T_i$ in the same grouping.

We will now count the amount of unknown coefficients left over after eliminating one per grouping. In a set $T_i$, the greatest possible exponent of $y$ and thus of $t$ is $(n+1)-i$. However, because we can only group terms with degrees in $x$ less than $n$, $(i+r) < n \Rightarrow r < (n-i)$ for any $G_{i,r}$, implying at most $n-i$ groupings per $T_i$ (from $r=0$ to $r = n-i-1$). The lower degree bound for terms in $T_i$ and for groupings, however, is the same: $\kappa(i,0)x^i \in T_i$ and terms in $G_{i,0}$ have degree $i$. Because we have every exponent of $y$ from 0 to $(n+1)-i$ in $T_i$, there are $(n+2)-i$ unknown coefficients and $n-i$ groupings per $T_i$, implying that there are 2 unknown coefficients left over after we eliminate one per grouping, as desired (we have excluded the special possibility that $i = n+1$, which would make $n-i$ impossibly negative). □

Now that we have proved Proposition 6.1, we will count the total number of unknown coefficients we have left over after eliminating as many as possible.

If the degree $n+1$ of $Q_n$ is odd, we do not have to worry about the case where the exponent $i$ of $x$ is equal to $n+1$ (all exponents of $x$ are even). Since there are $n/2$ even numbers greater than 0 (since $x^0$ already represents the quantity $(y-p_n)^n(y-p_s)$) and less than $n+1$, we have $n/2$ sets $T_i$. 2 unknown coefficients per $T_i$ yields $n$ total unknown coefficients. We have a total of $3n+3$ edges of our domain (Property 3). We have used $n+1$ edges perpendicular to $y$-axis, leaving us with $2n+2$ edges. Accounting for each remaining edge's symmetric counterpart, we have $\frac{2n+2}{2} = n+1$ edges to give us $n+1$ poles to set up $n+1$ equations to solve for the $n$ unknown coefficients. Since $n$ is even, we have a line that is tangent to the frozen boundary at an even amount of points, meaning that we can translate our domain so that a vertex lies on the origin. Then, we can use the homogenization technique used with $\Omega_4' \in \Omega_4$ (Section 6.1) to simplify the problem to $n$ equations with $n-1$ unknowns. Notice that when $n=4$, we will have 4 equations with 3 unknowns, the result achieved in Section 6.1.

If the degree $n+1$ of $Q_n$ is even, we apply a similar approach. There are $\frac{n-1}{2}$ even numbers greater than 0 and less than $n+1$, yielding $n-1$ unknown coefficients. However, there is also the case where the exponent of $x$ is $n+1$. Based on Proposition 6.1, this will add one more unknown coefficient to make the total $n$. Using the same logic as in the last paragraph, we have $n+1$ edges to give us $n+1$ poles to set up $n+1$ equations to solve for the $n$ unknown coefficients. Notice that when $n=3$, we will have 4 equations with 3 unknowns, the result achieved in Section 5.

An interesting note: for domains in any set $\Omega_n$, including $\Omega_1$ and its hexagons, we have had one more equation than the number of unknowns for which to solve. This indicates that any transposition of an edge (and the symmetric transposition of its symmetric counterpart for domains where $n \geq 2$) that could give one of these equation would destroy the tilability of the related domain. This is because the supposed frozen boundary, determined from the algorithms with an exclusion of the equation determined from the transposed edge, would not be tangent to that edge. This violates Property 1.

# 7 Conclusion

The problem of explicitly computing the frozen boundary for any tilable domain is a topic of great interest. It is interesting to note that in our computations, Properties 1, 2, and 3 were the only ones necessary to yield a unique curve. Other computations will require Property 4 in addition to the other 3 to create this uniqueness. Nevertheless, the other 3 properties alone create fruitful algorithms for the computation of the frozen boundaries contained in any of our considered tilable domains.

# 8 Acknowledgements

The author would like to thank his mentor Alisa Knizel for providing indispensable resources for progress in his research as well as for steering him in the right directions, listening to his ideas, and providing feedback for this paper. The author would also like to thank Professor Gorin for providing the project and for his feedback. The author would like to thank both of them for taking the time to talk to him personally about the project.

The author would like to thank Dr. Khovanova for offering valuable tips on writing quality papers and making quality presentations, as well as taking the time to meet with him personally concerning his project and presentation.

Also, the author is grateful for the MIT-PRIMES program for providing the opportunity to work on this project, and the author would like to thank Dr. Gerovitch for directing the program and Dr. Etingof for being the chief research advisor.

# References

[1] B. Bollobas, O. Riordan. Percolation. *Cambridge Univ. Pr.*, 2006.

[2] A. Borodin, V. Gorin, E. M. Rains. q-Distributions On Boxed Plane Partitions. *Selecta Mathematica, New Series, 16*, no. 4, 731–789, 2010. `http://arxiv.org/pdf/0905.0679v2.pdf`.

[3] H. Cohn, R. Kenyon, J. Propp. A Variational Principle for Domino Tilings. *Journal of the AMS 14*, 297-346, 2001. `http://arxiv.org/pdf/math/0008220v3.pdf`

[4] B. Duplantier and S. Sheffeld. Liouville quantum gravity and KPZ. *Invent. Math.*, 185(2):333–393, 2011.

[5] I. M. Gelfand, M. Kapranov, A. Zelevinsky. Discriminants, Resultants, and Multidimensional Determinants. *Birkhauser*, 2008. Print.

[6] V. Gorin. *Vadim Gorin's professional homepage.* `http://www.mccme.ru/~vadicgor/Random_tilings.html`.

[7] P. Griffiths, J. Harris. Principles of Algebraic Geometry. *Wiley-Interscience*, 1994. Print.

[8] G. Grimmett. Percolation. *Springer Verlag*, 1999.

[9] G. Hite, T. Zivkovic, D. Klein. Conjugated circuit theory for graphite. *Theor. Chim. Acta*, 74:349-361, 1988.

[10] W. Jockusch, J. Propp, P. Shor. Random domino tilings and the arctic circle theorem. *Unpublished manuscript*, 1995. `http://arxiv.org/pdf/math/9801068v1.pdf`

[11] P.W. Kasteleyn. Graph theory and crystal physics. Graph Theory and Theoretical Physics. *Academic Press. London*, 43-110, 1967.

[12] R. Kenyon, A. Okounkov Limit shapes and the complex Burgers equation, *Acta Mathematica*, December 200s, Volume 199, Issue 2: 263-302. `http://arxiv.org/pdf/math-ph/0507007v3.pdf`.

[13] R. Kenyon, A. Okounkov, Sc. Sheffield. Dimers and amoebae. *Ann. of Math.* (2), 163(3):1019 1056, 2006.

[14] H. Kesten. Percolation theory for mathematicians. *Birkhuser*, 1982.

[15] D. Klein, G. Hite, W. Seitz, T. Schmalz. Dimer coverings and Kekule structures on honeycomb lattice strips. *Theor. Chim. Acta*, 69:409-423, 1986.

[16] M. Monks. Duality of Plane Curves. `https://math.berkeley.edu/~monks/papers/DualityV3.pdf`.

[17] A. Okounkov. Limit shapes, real and imaginary. `http://www.math.columbia.edu/~okounkov/AMScolloq.pdf`.

[18] L. Petrov. Asymptotics of Random Lozenge Tilings via Gelfand-Tsetlin Schemes, *Probability Theory and Related Fields*, 160, no. 3, 429–487, 2001. `http://arxiv.org/pdf/1202.3901v2.pdf`.

[19] L. Petrov. Integrable Probability: Random Polymers, Random Tilings, and Interacting Particle Systems. `http://faculty.virginia.edu/petrov//research_files/talks/integrable.pdf`

[20] J. R. Sendra, F. Winkler, S. Perez-Diaz. Rational Algebraic Curves: A Computer Algebra Approach. *Springer Berlin Heidelberg*, 2007.

[21] W. P. Thurston. Conways tiling groups. *Amer. Math. Monthly*, 97(8):757-773, 1990.

[22] B. de Tiliere. The Dimer Model in Statistical Mechanics. *Laboratoire de Probabilites et Modeles Aleatoires, Universite Pierre et Marie Curie, Paris, France.* `http://proba.jussieu.fr/~detiliere/Cours/polycop_Dimeres.pdf`

[23] W. Werner, Lectures on two-dimensional critical percolation. *Statistical mechanics*, Vol. 16 of IAS/Park City Math. Ser., Amer. Math. Soc., Providence, RI, pp. 297-360, 2009. `http://arxiv.org/pdf/0710.0856v3.pdf`

[24] W. Werner. Percolation et modele d'Ising. Cours specialises. *SMF*, 16, 2009.